frontiers in Earth Science

ORIGINAL RESEARCH
published: 05 April 2019
doi: 10.3389/feart.2019.00069

Composition Systematics in the Exoskeleton of the American Lobster, *Homarus americanus* and Implications for Malacostraca

Sebastian T. Mergelsberg, Robert N. Ulrich, Shuhai Xiao and Patricia M. Dove*

Department of Geosciences, Virginia Polytechnic Institute and State University, Blacksburg, VA, United States

Studies of biominerals from the exoskeletons of lobsters and other crustaceans report chemical heterogeneities across disparate body parts that have prevented the development of composition-based environmental proxy models. Anecdotal evidence, however, suggests underlying composition systematics may exist in the mineral component of this biocomposite material. We test this idea by designing a protocol to separately extract the mineral [amorphous calcium carbonate (ACC) plus calcite] and organic (chitin plus protein) fractions of the exoskeleton. The fractions were analyzed by ICP-OES and other wet chemistry methods to quantify Mg, Ca, and P contents of the bulk, mineral, and organic matrix. Applying this approach to the exoskeleton for seven body parts of the American lobster, *Homarus americanus*, we characterize the chemical composition of each fraction. The measurements confirm that Mg, P, and Ca concentrations in lobster exoskeletons are highly variable. However, the ratios of Mg/Ca and P/Ca in the mineral fraction are constant for all parts, except the chelae (claws), which are offset to higher values. By normalizing concentrations to obtain P/Ca and Mg/Ca, we show that all body parts conserve P/Mg to 1.27 ± 0.30. The findings suggest lobsters hold promise as a novel class of animals that record composition systematics within their $CaCO_3$ biominerals. Parallel structural analyses of the bulk samples confirm a large proportion of ACC relative to calcite in the mineral fractions for each body part using high-energy X-ray diffraction and PDF analysis. There is no evidence for a phosphate phase. Returning to compositions reported for other marine (crab, lobster, and marine shrimp) and terrestrial (pillbug) crustaceans, we find evidence for similar Mg/Ca and P/Ca patterns in these organisms. The relationships provide a basis for developing new proxies for environmental reconstructions using animals from the class Malacostraca and provide insights into how composition may be optimized to meet functional requirements of the mineral fraction in exoskeletons. Compositional variability, and hence differential solubility, suggests a thermodynamic basis for the taphonomic bias that is observed in the fossil record.

Keywords: biomineralization, calcium carbonate, amorphous calcium carbonate, ACC, taphonomy, crustaceans, American lobster

OPEN ACCESS

Edited by:
Aleksey Sadekov,
The University of Western Australia, Australia

Reviewed by:
Bronwen Cribb,
The University of Queensland, Australia
Shmuel Bentov,
Ben-Gurion University of the Negev, Israel

****Correspondence:***
Sebastian T. Mergelsberg
sebastian.mergelsberg@pnnl.gov

Specialty section:
This article was submitted to Biogeoscience, a section of the journal Frontiers in Earth Science

Received: *10 December 2018*
Accepted: *19 March 2019*
Published: *05 April 2019*

Citation:
Mergelsberg ST, Ulrich RN, Xiao S and Dove PM (2019) Composition Systematics in the Exoskeleton of the American Lobster, Homarus americanus and Implications for Malacostraca. Front. Earth Sci. 7:69. doi: 10.3389/feart.2019.00069

INTRODUCTION

The American lobster (*Homarus americanus*) is a large decapod crustacean with a close evolutionary relationship to crabs, both of which belong to the class Malacostraca. All malacostracans possess an exoskeleton, a unique biomineral that provides protection and stability. With the realization that many taxa utilize amorphous calcium carbonate (ACC) during biomineralization, the lobster exoskeleton is a biomineral of particular interest. The structures are a biocomposite of organic matrix (60–80%) and $CaCO_3$ minerals (20–40%) as ACC and calcite (Roer and Dillaman, 1984).

As the most abundant component of the exoskeleton, the organic matrix is predominantly chitin with the remainder as protein (≈5–7%) and small organic molecules. The primary function of the organic matrix is to provide a framework during the intermolt period while the calcium carbonate is postulated to add rigidity and the ability to withstand higher impact forces. Both of these phases may have additional complementary functions such as maintaining osmotic balance or inhibiting infection (Glynn, 1968; Greenaway, 1985; Kunkel et al., 2012). Compared to arthropods that use chitin exclusively, such as the insects and chelicerates, crustaceans can grow larger, highly diverse body structures including claws, and swimming tails. The consistent constitution of the exoskeleton, despite variable body size, morphology, and function across crustacean species (Roer and Dillaman, 1984), suggests a highly regulated biomineralization process.

This study is focused on characterizing the chemical patterns contained in the amorphous and crystalline phases of calcium carbonate, which we collectively refer to as the mineral component. Approximately 80 to 95% of the mineral fraction is composed of ACC and this metastable polymorph persists without transforming to crystalline products for up to a year between molting cycles (Hayes and Armstrong, 1961). This persistence of ACC contrasts with most animals that use ACC as a short-lived intermediate that transforms within a few hours to days to the subsequent crystalline biomineral products (Aizenberg et al., 1996; Addadi et al., 2003). With its large size and long molting cycles, the lobster thus provides an ideal model organism to characterize biogenic ACC properties and provide insights into the material-function relationship of exoskeletons.

Previous studies that investigated origins of ACC metastability focused on the quantity of Mg and P (from phosphate) as elements that are known to modify $CaCO_3$ properties and are abundant in biological systems (Levi-Kalisman et al., 2002; Akiva-Tal et al., 2011; Sato et al., 2011). The direct relationship between Mg content and ACC lifetime is well-documented (Loste et al., 2003; Blue et al., 2017), but the role of P is not well understood. *In vitro* studies show P stabilizes ACC and slows its transformation into crystalline polymorphs for several hours (Reddy, 1977; Clarkson et al., 1992; Bentov et al., 2010). In contrast, ACC transforms to crystalline products within seconds to minutes in pure $CaCO_3$ compositions (Sawada, 1997; Blue et al., 2017). To achieve the longevity of ACC that is observed in many crustaceans, these observations suggest both Mg and P have stabilizing roles.

Amorphous calcium carbonate can also be stabilized by interactions with biomacromolecules (Aizenberg et al., 1996). Traditionally, the scientific community has assumed that aspartic and glutamic acid sidechains of proteins are the primary moieties involved in lowering the energetic barrier to ACC nucleation (Addadi et al., 2006). Recent work, however, shows that other functional groups may also promote ACC precipitation and prevent particle dissolution (Arias and Fernandez, 2008; Qi et al., 2014). An interplay of cations and macromolecules to stabilize ACC is also plausible. For example, Mg is often involved in the ionic stabilization of protein structures (Glusker, 1991), while phosphate groups are common and often covalently attached to serine and threonine sidechains (Bentov et al., 2010). These observations raise the question whether P is primarily associated with the mineral or organic components of the exoskeleton. It is possible that P is concentrated in the protein component, yet still able to influence the stability of mineral fraction.

A number of studies report the compositions of exoskeletons from Malacostraca animals (**Table 1**), but a consistent picture of biomineral chemistry has not emerged. This lack of a chemical framework for interpreting, and thus predicting, exoskeleton properties has limited the usefulness of these animals as indicators of environmental and physiological conditions. There are several obstacles to advancing this knowledge. First, most studies report the composition of the *bulk* exoskeleton, an average of contributions from mineral and organic constituents. It is possible the large organic fraction masks unrecognized systematics in mineral composition. To our knowledge, one study reports compositions of the separated mineral fraction (ACC + calcite) for the lobster cephalothorax and shows Mg and P are concentrated in the ACC component (Levi-Kalisman et al., 2002). This raises the second point that most investigations are limited to specific body parts, not all of which are homologous amongst all crustaceans. Third, most studies did not quantify concentrations of all three elements. Finally, many studies use small sample sizes to control for variations in composition that are influenced by differences in local temperature, food availability, molting cycles, and other environmental and biological variables.

Although the data are limited, **Table 1** contains anecdotal evidence that exoskeleton compositions are body part-specific and there may be an underlying relationship between Mg, P, and Ca. For example, the larger crustaceans (e.g., lobsters and crabs) generally show higher Mg and P levels than shrimp. Evidence from these bulk measurements, combined with advances in understanding chemical controls on ACC stability, lead us to hypothesize that the lobster exoskeleton has body part-specific compositions that may reflect broader systematics. To test this idea, we designed a protocol to separately extract the organic and mineral fractions of seven body parts from two lobsters. These fractions were analyzed by

TABLE 1 | Summary of studies reporting the P and Mg content of the American lobster and other decapod exoskeletons.

Organism	Bulk Mg wt%	Bulk P wt%	Body parts	Reference and notes
American Lobster,	1.46%	2.41%	Chela	Clarke and Wheeler, 1922 [a]
H. americanus	1.11%	1.65%	Cthx	Clarke and Wheeler, 1922 [a]
	N/A	0.88–1.82%	Cthx	Travis, 1963 [b]
	10%*	12%*	Cthx	Levi-Kalisman et al., 2002 [c]
	1.2%	0.65%	Chela	Boßelmann et al., 2007 [d]
	1.0%	2.1%	Cthx	Boßelmann et al., 2007 [d]
	0.60%	0.99%	Chela	This study
	0.37%	0.52%	Thx	This study
	0.45%	0.67%	Legs	This study
	0.47%	0.63%	Ceph	This study
	0.39%	0.62%	Abd	This study
	0.33%	0.57%	Upd	This study
Blue crab, *C. sapidus*	2.2%	N/A	Cthx	Vigh and Dendinger, 1982
Red rock crab,	1.4%	0.9%	Chela	Boßelmann et al., 2007 [e]
C. pagurus	1.2%	1.1%	Cthx	Boßelmann et al., 2007 [e]
California brown shrimp,	1.23%	1.93%	Rost	Huner et al., 1979 [f]
P. californiensis	0.99%	1.86%	Cthx	Huner et al., 1979 [f]
	0.61%	1.32%	Abd	Huner et al., 1979 [f]
Indian white prawn,	1.2%	1.2%	Av	Vijayan and Diwan, 1996 [g]
P. indicus	2.8%	<1.2%	Rost	Vijayan and Diwan, 1996 [g]
	0.4%	>1.2%	Swrt	Vijayan and Diwan, 1996 [g]
Woodlouse, *P. scaber*	0.71%	0.69%	Cpce	Becker et al., 2005
Pillbug, *A. vulgare*	0.72%	0.59%	Cpce	Becker et al., 2005

[a] Averages for three animals; [b] Highest and lowest concentrations recorded throughout molt cycle; [c] ACC fraction only; [d] Highest concentration of P found in cephalothorax; [e] Red rock crab, C. pagurus. This species has a very thick exoskeleton; [f] Most comprehensive bulk and mineral data; [g] Quantified elemental distribution across body parts during the molt cycle. Cthx, cephalothorax; Ceph, cephalon; Thx, Thorax; Abd, abdomen; Upd, uropod; Rost, rostrum; Av, average; Swrt, swimmerets; Cpce, carapace. See ***Supplementary Table S1*** *for average concentrations for each body part.*

wet chemistry methods to quantify the Mg, Ca, and P content of the bulk, mineral, and organic matrix. A parallel structural analysis of the mineral samples determined the proportions of ACC and calcite.

MATERIALS AND METHODS

Animal and Sample Preparation

Live specimens of *H. americanus* used in this study were captured at Point Judith, Rhode Island (Lobster Guy, online retailer), shipped to our laboratory, and flash frozen for 30 min at −80°C within 1 h of receipt. The animals were adult males in the C4 stage of intermolt and collected during early summer. Sample preparation began by thawing both animals at room temperature for ≈2 h and dissecting them in air. Exoskeleton samples were prepared from two animals in sets of three (sampling triplets) for each body part of interest (**Figure 1**), a total of six samples for each body part. Each of these samples was subsequently analyzed in triplicate to give a total of 18 measurements per body part. The exoskeleton samples were then rinsed for 5 s in 18.2 MΩ·cm ultrapure water and methanol and dried in air. When processing occurred on another day, the exoskeleton samples were put into sealed polystyrene containers and stored in a freezer at −20°C. Each sample was frozen in liquid nitrogen and ground to a homogenous powder in a mortar and pestle in preparation for component dissolutions.

Dissolution of the Organic and Mineral Fractions

The experimental design used three extraction procedures to isolate the mineral (ACC plus calcite) fraction from the organic (separate chitin and protein) fraction. To dissolve the mineral fraction, each bulk powder was individually weighed and decalcified in 10% acetic acid at 4°C for 24 h. The supernatant was collected via vacuum filtration on polyethersulfone (PES) filters (<30 nm; Sterlitech, Kent, WA, United States) and stored at 4°C until analysis. The remaining solids were rinsed in 18.2 MΩ·cm ultrapure water for 25 s, then rinsed for 25 s in methanol, dried in air, and weighed.

The water-soluble proteins in the exoskeleton were dissolved by adding the residual decalcified sample to a solution of 6 M urea and 0.06 M Tris at pH 6.3. Dissolution occurred for 24 h at 4°C, followed by separation by vacuum filtration. Each sample was collected and stored at 4°C for later analysis. Remaining solids were rinsed in 18.2 MΩ·cm ultrapure water for 25 s, for 25 s with methanol, dried in air, and weighed.

In a final step, the powders were added to a 10 M HCl solution for a minimum of 24 h to dissolve the chitinous samples completely. Bulk concentrations were calculated using the sum

of elements removed by each dissolution procedure divided by the initial weight of each sample. Element concentrations are reported only for the total organic matrix because of the analytical errors associated with measurements of the small amount of protein relative to chitin. **Supplementary Table S1** summarizes the wt% of the mineral fraction for each body part of the exoskeleton.

Composition Analysis

Effluents from the three separation procedures were analyzed via ICP-OES to measure the total concentrations of Ca, Mg, and P in the collected solutions. Analyses were performed using a Spectro® ARCOS SOP instrument using an yttrium internal standard. Reference solutions were prepared independently to exclude impurities from the solvents used in each extraction. For each sample, the resulting solutions were split into thirds to provide instrumental triplets, such that 18 measurements were made for each body part. Detection limits for Ca and Mg were 0.033 and 0.079 mg/L for P. Error estimates for these analyses are reported as the 1σ standard error from triplicate analyses.

Pair Distribution Function (PDF) Analysis

The predominance of ACC in the mineral fraction (Wood and Russell, 1987) was confirmed by characterizing the crystallinity using x-ray diffraction at the Advanced Photon Source (Argonne, IL, United States) using beamline 11-ID-B (Rütt et al., 2001) and an incident photon energy of ~58.6 keV (λ = 0.2114 Å). Samples of bulk exoskeleton were mounted between two opposing pieces of polyimide (Kapton®) tape and the scattered radiation was measured in transmission mode using an amorphous-Si detector system manufactured by Perkin Elmer™ (2048 × 2048 pixels, 200 × 200 μm^2 pixel size). A CeO_2 standard (NIST diffraction standard set 674a) was used to calibrate the sample-to-detector distance and the non-orthogonality of the detector relative to the incident beam path. Conversion of scattering data from 2D to 1D was performed using the program Fit2D (Hammersley et al., 1995). A polarization correction was applied during integration of the data. Direct subtraction of the sample holder was accomplished by the independent measurement of the true background intensity of a blank polyimide tape. PDF analysis profiles were calculated using PDFgetX2 (Qiu et al., 2004).

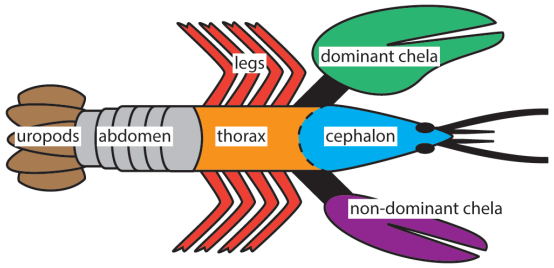

FIGURE 1 | The seven body parts of *H. americanus* investigated in this study. Three or more samples were collected from each location while also distinguishing between the distal and proximal sites on the chela for a total of 30 exoskeleton samples per animal.

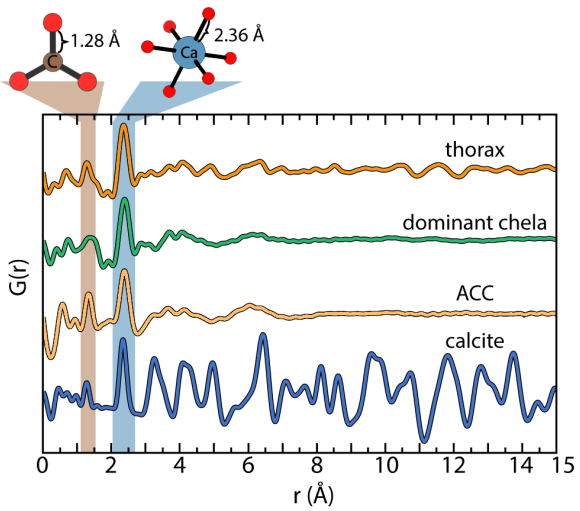

FIGURE 2 | Characteristic pair distribution function (PDF) analysis determined for the reference standards (Michel et al., 2008) and the bulk fraction of the thorax and dominant chela. The similar profiles of amorphous calcium carbonate (ACC) and the dominant chela indicate the predominance of ACC. Linear analysis of the PDF data estimate the mineral component of the thorax and dominant claw is ≈85 and ≈97% ACC, respectively, with the remainder as calcite.

The proportion of crystalline and ACC as calcite and ACC were determined using linear analysis to fit synthetic standards (Michel et al., 2008) to sample PDF profiles.

RESULTS

Mineral Component Is Primarily ACC

Pair distribution function analyses of the high-energy x-ray scattering data confirm the mineral fraction of the exoskeleton contains ACC and calcite in variable proportions between body parts (Hayes and Armstrong, 1961; Al-Sawalmih et al., 2009). For example, the thorax is ≈86% ACC in contrast to the chelae with ≈97% ACC. The short-range order of the biogenic ACC is consistently ≈7Å and calcite particle diameters are well above 1.5 nm (**Figure 2**). There is no structural evidence for a separate phosphate or other amorphous or crystalline phases in any of the body parts (see later Discussion).

Mineral Fraction Contains Variable Mg, P, and Ca Levels With Constant Ratios

The Mg concentration in the mineral fraction (ACC plus calcite) varies across the exoskeleton with differences of up to ≈5× between the seven body parts (**Figure 3A**). The legs and abdomen exhibit the largest variability, while the uropods and thorax have relatively uniform compositions. Despite differences in total concentrations, Mg and Ca are covariant across all body parts, except the chelae, by the relation:

$$(\text{wt\%Mg}) = 0.087(\text{wt\%Ca}) - 0.040 \qquad (1A)$$

The near zero intercept of Eq. 1A allows us to assume the slope of 0.087 is approximately equal to the Mg/Ca of the exoskeleton for all body parts. To put this into perspective, the seawater habitat of the lobster has Mg/Ca ≈5. Chelae compositions are offset to greater Mg concentrations to give:

$$\text{wt\%Mg}) = 0.073(\text{wt\%Ca}) + 1.022 \quad (1B)$$

where R^2 = 0.896 across 12 measurements (e.g., **Supplementary Table S1**). Statistics for these relationships and the entire body are reported in **Supplementary Table S3**.

Total phosphorous concentration is also variable between body parts, but again, P levels are covariant with Ca (**Figure 3B**). For all body parts except the chela, the relationship between P and Ca concentrations is given by:

$$(\text{wt\%P}) = 0.087\ (\text{wt\%Ca}) + 0.188 \quad (2)$$

The phosphorous contents of the chelae are offset to higher values by ≈30% (for three claw samples) without an apparent trend (**Supplementary Tables S1, S3**); except for greater P levels measured in the distal part of the claw (toward the tip). P concentrations in the proximal parts of both claws are similar to other body parts.

As expected from **Figures 3A,B**, the relationship between P and Mg in **Figure 3C** is conserved for all body parts, except the chelae:

$$(\text{wt\%P}) = 1.00\ (\text{wt\%Mg}) + 0.16 \quad (3A)$$

A similar dependence is determined for the ensemble of all body parts:

$$(\text{wt\%P}) = 1.11\ (\text{wt\%Mg}) + 0.11 \quad (3B)$$

where R^2 = 0.825 across all measurements. To our knowledge, a P/Mg correlation is not previously reported in carbonate biominerals, but the statistical analyses show high certainty with very low standard errors and *p*-values (**Supplementary Table S3**). By themselves, the chelae do not exhibit a clear relationship between Mg and P.

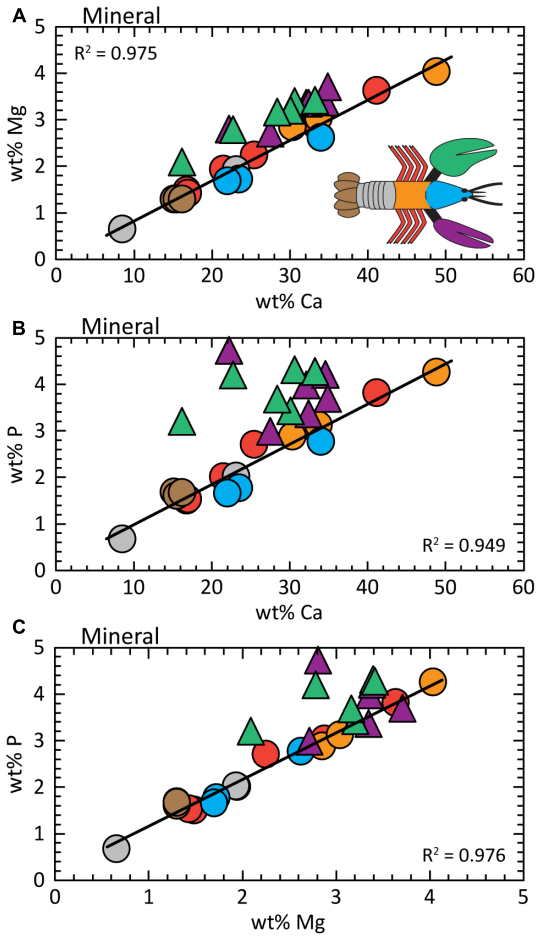

FIGURE 3 | Analysis of the mineral fraction shows element concentrations are covariant; chelae compositions are offset to higher wt% Mg and wt% P. **(A)** wt% Ca vs. wt% Mg; **(B)** wt% Ca vs. wt% P; **(C)** wt% Mg vs. wt% P. Regression fits are determined for the data from all body parts except the chelae. Detailed statistics are presented in **Supplementary Table S3**.

Average Composition of the Mineral Fraction

Recognizing that the biomineral is a polymorphic mixture of ACC and calcite that cannot be physically separated, we estimate an average composition. The mineral fraction in the thorax exhibits a solid-solution with the average composition:

$$Ca_{0.850}Mg_{0.072}\ [H,\ Na,\ K]_{0.078}\ (CO_3)_{0.922}\ (PO_4)_{0.078} \quad (4A)$$

Chelae (for both claws) contain more Mg and P relative to Ca as given by:

$$Ca_{0.801}Mg_{0.088}\ [H,\ Na,\ K]_{0.111}\ (CO_3)_{0.889}\ (PO_4)_{0.111} \quad (4B)$$

These compositions were determined using all of the mineral fraction analyses in this study. We also assume: (1) all measured elements are associated with a single phase, (2) mineral composition is charge-balanced by substitution of expected monovalent cations (Na^+, K^+, and H^+), and (3) P occurs as PO_4^{3-}. The speciation of anions and concentrations of monovalent cations were not measured, thus the nature of the charge-balance substitution is unknown. Previous studies assume the presence of hydroxide (Becker et al., 2005; Kunkel et al., 2012), but a high concentration of this anion seems unlikely given that local conditions during exoskeleton deposition are not expected to exceed pH 9 (Ziegler, 2008).

We assume the amorphous polymorph contains a greater proportion of Mg and P relative to the calcite (Dai et al., 2008; Sato et al., 2011; Blue et al., 2017). This is consistent with structural (**Figure 2**) and chemical (**Figures 3A,B**) data determined for the chelae versus thorax.

Low Levels of Mg P, and Ca in the Organic Fraction

The organic matrix contains very low concentrations of Mg, P, and Ca compared to the mineral fraction (compare axis values

in **Supplementary Figure S1** and **Figure 3**). All linear regression models show a statistically significant correlation between element concentrations ($p < 0.05$), but the low Mg values in the organic fraction are within the error of the larger concentrations measured for the mineral fraction (**Supplementary Figure S1A** and analysis in **Supplementary Table S3**). Similarly, the organic portion of most exoskeleton parts contains low wt%P (less than 0.1, **Supplementary Figure S1B**), which also has a minor impact on bulk composition relative to the mineral fraction. The very high *ratios* of P/Ca and P/Mg in the organic fraction are likely due to contributions by phosphorylated peptides.

The absence of a distinct composition signature in the organic fraction is illustrated in **Figure 4A**. Mg/Ca ratios determined for the organic matrix are widely dispersed relative to the narrow range of values in the mineral fraction (gray band). We acknowledge the disparate values obtained for the organic fraction include analytical errors associated with measurements near the detection limit of our analysis. The P/Ca (**Figure 4B**) and P/Mg (**Figure 4C**) ratios show similarly wide dispersions for the organic fraction compared to the mineral.

Bulk Exoskeleton Composition Dominated by the Mineral Fraction

Although the organic fraction dominates the volume and mass of the bulk exoskeleton, bulk composition trends mimic those of the mineral fraction (compare **Figures 5A–C**, **3**). Similarities include offsets of the chelae to higher Mg and P concentrations. This is supported by the conserved Mg/Ca and P/Ca ratios in the mineral fraction of the chelae and the rest of the body, respectively (**Figures 4A,B**). Absolute concentrations are lower due to the "dilution" effects of the large organic fraction. Our finding that the mineral fraction is the driver to bulk composition is illustrated by comparing the normalized elemental ratios of the bulk and mineral components (**Figures 5D–F**). All ratios exhibit a 1:1 dependence with high statistical confidence (**Supplementary Table S3**). The findings confirm the assumption of previous studies that bulk exoskeleton composition can be used to infer biomineral composition for the elements investigated herein. However, element ratios are more useful as indicators of composition for bulk and mineral fractions because of the variable concentrations that occur both within and between body parts.

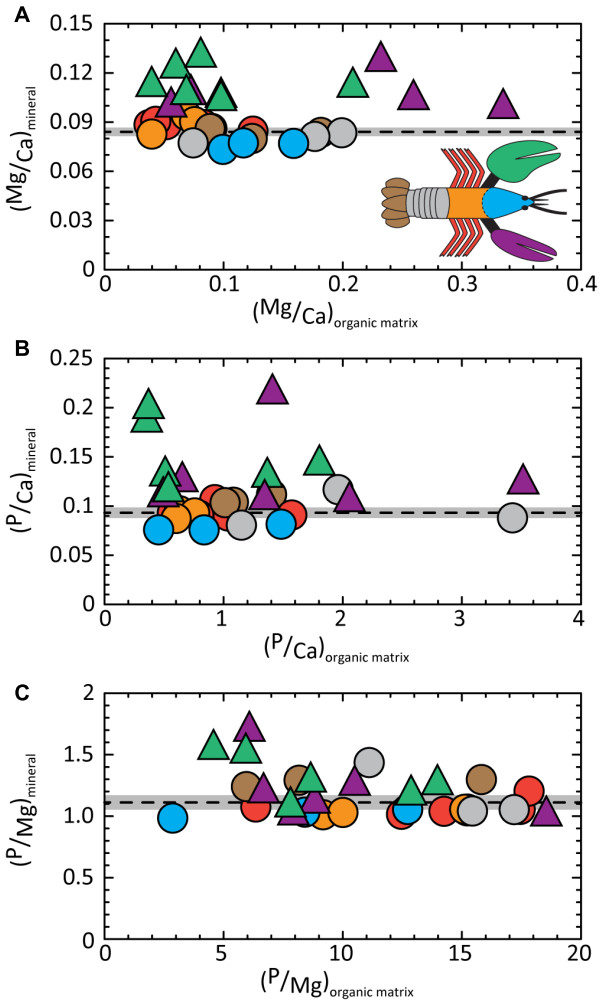

FIGURE 4 | Molar ratios of elements contained in the mineral fraction of exoskeleton body parts are conserved relative to the wide range of ratios determined for the corresponding organic fraction. Dashed lines give average values of **(A)** $(Mg/Ca)_{mineral} = 0.084 \pm 0.001$; **(B)** $(P/Ca)_{mineral} = 0.093 \pm 0.003$; and **(C)** $(P/Mg)_{mineral} = 1.110 \pm 0.030$. Gray bands illustrate the 2σ standard error (95% confidence interval). Detailed statistics are given in **Supplementary Tables S1, S3**.

DISCUSSION

Chemistry of Mineral Component Is Highly Regulated

Our finding that Mg/Ca and P/Ca are conserved in the exoskeleton (**Figures 4A,B**) is consistent with previous studies implicating these ions in optimizing $CaCO_3$ properties. The data also indicate the lobster joins other biomineralizing animals, such as echinoderms and mollusks in their ability to produce characteristic biomineral compositions. For example, the Mg/Ca ratio is well-established for shells of many bivalves (Klein et al., 1996; Freitas et al., 2006).

There are three plausible explanations for why regulating Mg and P concentrations confers physical and chemical advantages to exoskeleton function. First, studies show that increasing concentrations of Mg and P increase the lifetime of the metastable amorphous polymorph optimize proportions of ACC to calcite for the duration of the molt cycle. Also, *in vitro* studies show Mg and P also progressively modify ACC morphology (Xu et al., 2005; Blue and Dove, 2015). In contrast to the more uniform size and shape of impurity-free ACC particles, incorporation of Mg or P produces more variably sized aggregated spheroids (Xu et al., 2005; Blue and Dove, 2015). It is plausible that ACC allows for greater morphological and functional diversity within the composite material.

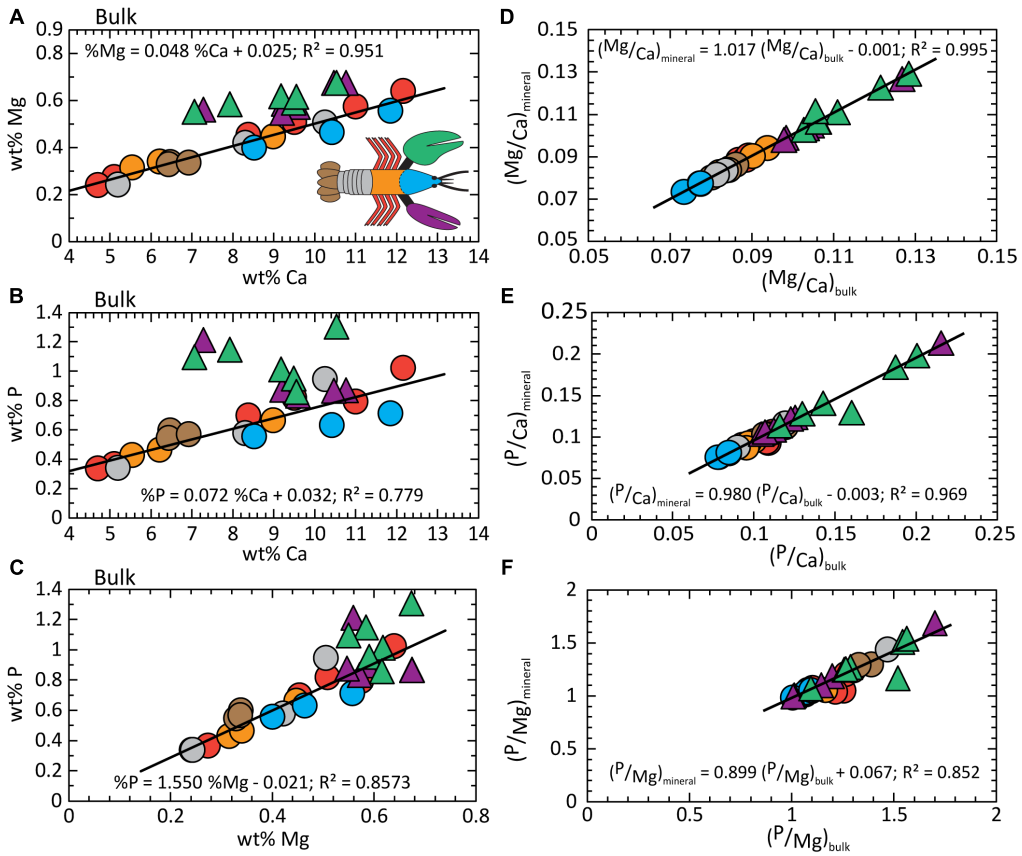

FIGURE 5 | Composition analysis of the bulk exoskeleton. **(A)** wt% Ca vs. wt% Mg; **(B)** wt% Ca vs. wt% P; **(C)** wt% Mg vs. wt% P. The 1:1 relationship between element ratios in the mineral fraction versus bulk exoskeleton demonstrates bulk composition is dominated by the contributions from the mineral. **(D)** Mg/Ca; **(E)** P/Ca; and **(F)** Mg/P. Detailed statistics are given in **Supplementary Table S3**.

Second, ACC is proposed to function as a chemical buffer (Kunkel et al., 2012). The exoskeleton has a critical role in maintaining the osmotic and ionic balance between the haemolymph of the animal and sea water (Glynn, 1968; Greenaway, 1985). An abundance of ACC particles may maintain this balance throughout the molt cycle. As a metastable phase, ACC also provides readily accessible buffering capacity in the event of exoskeletal damage (Kunkel et al., 2012).

Finally, previous studies suggest Mg and P promote bonding with the organic matrix to increase physical strength (Neues et al., 2007; Cribb et al., 2009). For example, P distribution at the submicron scale through the ACC may reflect differences in protein identity, degree of crosslinking, and the presence of glycoproteins (Marlowe et al., 1994; Coblentz et al., 1998). The skeletal structures of diverse animals show evidence for impurity-enhanced physical properties such as the Sr-rich aragonite in claws of the blue crab (Vigh and Dendinger, 1982) and Mg and P enriched carbonate mineral(s) from the puparial cuticle of the fly species, *M. autumnalis* and *M. domestica* (Grodowitz et al., 1987). In the latter example, Mg and P are thought to partially replace the sclerotization of organic cuticle components (Roseland et al., 1985). These studies suggest high concentrations of Mg and P are associated with body parts that require additional reinforcement. Other investigations report that greater levels of Mg, P, and other trace elements are found in high stress locations of specialized structures (Becker et al., 2005; Boßelmann et al., 2007). In these cases, however, local composition shifts are mostly attributed to the presence of other minerals.

No Evidence for a Separate Phosphate Phase

Previous studies debate the presence of amorphous and crystalline phosphate minerals in lobster exoskeletons. Examples include the phosphate phases associated with localized features, such as organule canals (Kunkel et al., 2012) and fluorapatite in proventicular teeth of both *H. americanus* (Bentov et al., 2016) and *C. quadricanrinatus* (crayfish; Bentov et al., 2012). Phosphate minerals have been identified in the exoskeleton of multiple malacostracans by studies that have characterized specialized exoskeleton structures (Becker et al., 2005; Boßelmann et al., 2007). Arguments for a separate phosphate phase that persists throughout the molting cycle are made for the giant prawn *M. rosenbergii* (Soejoko and Tjia, 2003). Some suggest incorporation of these

elements into the exoskeleton increases its physical strength without identifying any specific mechanisms (Neues et al., 2007; Cribb et al., 2009). Yet, other studies are unable to differentiate phosphate phases from high P carbonate mineral phases using high-resolution spectroscopy and Thermo-Gravimetric Analysis (Becker et al., 2005; Boßelmann et al., 2007; Al-Sawalmih et al., 2009).

In this quantitative study, structural analyses of the thorax and chelae detect only ACC and calcite, without evidence for additional inorganic phases (e.g., **Figure 2**). Moreover, a simple sensitivity analysis suggests the probability of a separate phase is low. First, stoichiometric P/Ca ratios of common calcium phosphate minerals are 0.6 to 2.0 for monocalcium phosphate $Ca(HPO_4)_2$ to the apatite family $Ca_5(PO_4)_3(OH)$, respectively. If one assumes all P is contained in a single and separate phase, the mineral fraction would need to contain ≈5 to 16% of this phase to give the P/Ca of 0.093 ± 0.003 determined in this study (**Figure 4B**). This amount is well above the 1 to 2% resolution of the PDF analysis for phosphate minerals. However, the limitations of current analytical methods prevent an unambiguous conclusion. For example, if P is distributed in multiple minor crystalline or amorphous phases, the detection of additional phase(s) in the total profile is further decreased. Knowledge of the exact structure(s) is also critical to detection.

Enigma of a P/Mg Signature

To our knowledge, the covariance of Mg and P in the exoskeleton of the main body and the chelae is not previously reported in biominerals. The relationships in **Figures 3A,B**, **4A,B** suggest an interplay between the concentration of these elements and calcium. To test this idea, we evaluate Mg and P concentrations, normalized to Ca. By comparing Mg/Ca and P/Ca ratios, **Figure 6A** shows the compositions of all body parts, including the chelae, collapse onto a single trend given by:

$$\left(\mathrm{P}/\mathrm{Ca}\right) = 2.03\left(\mathrm{Mg}/\mathrm{Ca}\right) - 0.07 \qquad (5)$$

As seen in **Figure 6A**, the relationship resolves the cephalon, posterior parts of the body, and chelae into distinct compositional regions. Rearranging Eq. 5 and substituting the bulk Ca/Mg value for all body parts (10.86 ± 0.29; **Supplementary Table S1**), we obtain the mean P/Mg signature of 1.27 ± 0.30 for the entire exoskeleton. This value is internally consistent with compositions (4A) and (4B) within the errors of the estimate.

Recalling that Mg and P have probable roles in increasing the lifetime of ACC, it is plausible the Mg/P signature has geochemical origins. For example, the relationship in **Figure 6A** could be explained by charge balance requirements. Owing to the relatively high charge density of Mg^{2+}, a coupled substitution between Mg^{2+} and HPO_4^{2-} may occur in the mineral fraction with phosphate groups substituting for CO_3^{2-}. Alternatively, the size difference between the small Mg^{2+} and larger Ca^{2+} may be the primary driver for substituting a portion of CO_3^{2-} by the larger HPO_4^{2-}. Arguments against a size-based interpretation include the fact that most of the mineral fraction is amorphous and therefore the typical rules for ion substitution should not apply. However, our structural analysis shows short-range ordering within 7 Å, suggesting the possibility of crystalline domains.

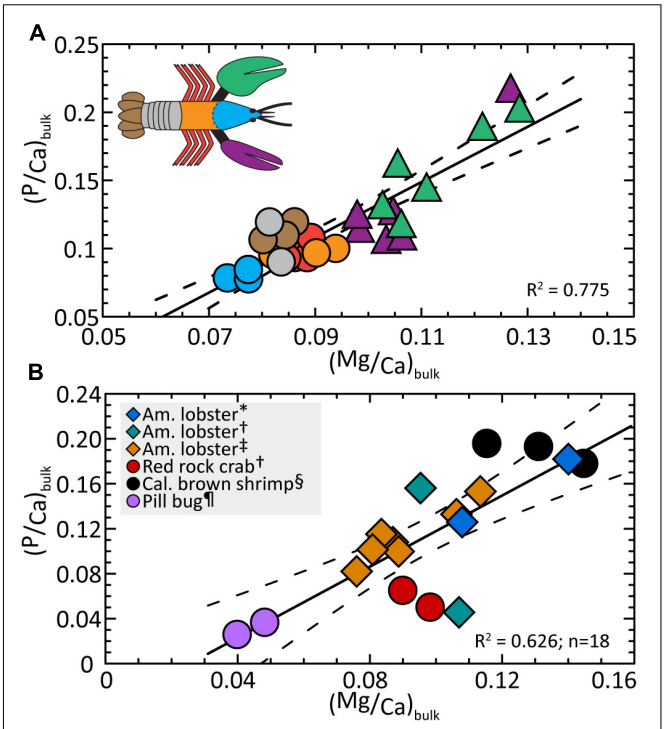

FIGURE 6 | (A) Ratios of P/Ca and Mg/Ca are covariant in the lobster bulk exoskeleton. Compositions indicate a linear trend that includes all body parts and also resolves the cephalon (head), main body, and claw compositions into distinctive ranges. Linear regression (Eq. 5) finds P/Mg is conserved at 1.27 ± 0.30 across all body parts. **(B)** The available exoskeleton data for other Malacostraca animals (**Supplementary Table S2**) are compared with measurements from this study (one averaged data point per body part) and show a similar interspecies correlation. Dashed lines correspond to the 2σ standard error (95% confidence interval) about the regression (solid line). Detailed statistics are given in **Supplementary Table S3**. *Clarke and Wheeler (1922), †Boßelmann et al. (2007), ‡ this study; § Huner et al. (1979), ¶ Becker et al. (2005).

Broader Pattern for Multiple Crustacean Species?

The relationships in **Figure 6A** lead us to return to the reported bulk compositions (**Table 1**) and ask if the exoskeletons of other crustacean species contain similar Mg/Ca and P/Ca systematics. We first assume bulk compositions of exoskeletons from other species are dominated by the mineral fraction as demonstrated in this investigation of the lobster. For those few studies that also report Ca data, we calculate bulk Mg/Ca and P/Ca. **Figure 6B** suggests the exoskeleton of three marine animals (crab, lobster, and marine shrimp) and one terrestrial species (pillbug) exhibit a similar composition trend for 17 measurements per animal:

$$\left(\mathrm{P}/\mathrm{Ca}\right) = 1.58\left(\mathrm{Mg}/\mathrm{Ca}\right) - 0.04 \qquad (6)$$

We recognize the available data are limited (**Supplementary Table S2**) and that we cannot account for modifying factors such as the dependence of composition on the age of an individual animal (Richards, 1951). We also note the calcite-enriched chelae of the red rock crab (Boßelmann et al., 2007) plot below the trend but this offset is consistent with our finding that lobster body parts with a greater fraction of calcite are associated with lower P/Ca. Rewriting Eq. 6 and substituting the ratio of Ca/Mg = 11.40 ± 1.0 for all animals (**Supplementary Tables S1, S2**), we obtain a P/Mg signature = 1.12 ± 0.04. The relationship suggests Mg and P levels may be co-optimized in the exoskeletons of each species to meet functional needs and indicates crustacean exoskeletons share previously unrecognized composition patterns.

Physical Basis for Taphonomic Bias in Skeletal Preservation

The fossil record of decapods is dominated by isolated chelae (Hyžný et al., 2015) and modern taphonomic studies conducted in the field and the laboratory indicate the chelae are sometimes the only skeletal elements to survive significant degradation and fragmentation (Allison, 1986; Mutel et al., 2008). Our measurements showing that chelae have a high P/Ca may provide a thermodynamic basis for empirical observations of a preservation bias for chelae compared to other skeletal elements— Substitution of P into the carbonate solid at concentrations near those observed in exoskeletons is known to significantly reduce the solubility and growth of carbonate phases (Avnimelech, 1983; Busenberg and Plummer, 1985). This reduced solubility may provide a thermodynamic basis for the taphonomic bias observed in the fossil record. As discussed previously, P interactions between mineral and organic matrix may also promote durability of this composite.

Findings from this study may also explain the observation that decapod fossils are preferentially preserved in phosphatic concretions (Tsujita, 2003). Ca and P from the degrading decapods could at least partially sustain phosphatization, as suggested by numerous studies of arthropod and vertebrate taphonomy (Martill, 1990; Briggs and Kear, 1994; Briggs and Wilby, 1996). There is some evidence to the contrary (Allison, 1986), but the findings of this study provide a path forward.

CONCLUSION

This investigation quantifies the composition of seven exoskeleton body parts of the lobster exoskeleton and shows that the chemical heterogeneities contain distinct signatures. For the two animals investigated in this study, the chelae exhibit Mg/Ca of 0.073 and 0.87 wt% for the chelae and all body parts, respectively. Similarly, P/Ca is also conserved at 1.0 and 1.11 wt % for the chelae and all body parts, respectively. Thus, the Mg and P concentrations demonstrate a constant P/Mg = 1.27 ± 0.3 for all body parts. To our knowledge, a P/Mg signature has not been previously identified in any carbonate biomineral and we do not postulate a biological or physical basis for this chemical pattern. The chemical pattern reiterates the highly regulated biomineralization processes that produce exoskeleton structures. Further, by applying our finding that bulk concentration of Ca, Mg, and P in the lobster exoskeleton is dominated by the mineral fraction, we return to published data and show evidence that other Malacostraca animals share similar Mg/Ca and P/Ca systematics. The relationships provide a chemical evidence for shared biomineralization processes across diverse marine and terrestrial crustaceans perhaps through their evolutionary roots. For example, the lobster is an early decapod species whose biomineralization pathways pre-date those of crabs and isopods (pillbugs, etc.,) while similar trends are noted across species in later decapods and malacostracans. The composition patterns, determined for two individual lobsters, reiterate the idea that diverse structure-function requirements of exoskeletons are optimized, at least partially, through composition. The relations suggest a new type of environmental reconstruction, based upon the lobster or close relatives, may be possible.

AUTHOR CONTRIBUTIONS

SM and PD designed the study. SM and RU performed the experiments. SM performed data analysis and statistical tests and wrote the first draft of the manuscript. PD, SX, and SM wrote sections of the manuscript. All authors contributed to revision and have read and approved the submitted version.

FUNDING

This project was funded by the United States DOE Office of Basic Energy Sciences Award BES-FG02-00ER15112 and used resources of the Advanced Photon Source, a United States Department of Energy (DOE) Office of Science User Facility operated for the DOE Office of Science by Argonne National Laboratory under Contract No. DE-AC02-06CH11357. X-ray scattering experiments were performed at beamline 11-ID-B by F. Marc Michel.

ACKNOWLEDGMENTS

The authors thank J. Donald Rimstidt for thoughtful comments and discussions.

SUPPLEMENTARY MATERIAL

The Supplementary Material for this article can be found online at: https://www.frontiersin.org/articles/10.3389/feart.2019.00069/full#supplementary-material

REFERENCES

Addadi, L., Joester, D., Nudelman, F., and Weiner, S. (2006). Mollusk shell formation: a source of new concepts for understanding biomineralization processes. *Chem. A Eur. J.* 12, 980–987. doi: 10.1002/chem.200500980

Addadi, L., Raz, S., and Weiner, S. (2003). Taking advantage of disorder: amorphous calcium carbonate and its roles in biomineralization. *Adv. Mater.* 15, 959–970. doi: 10.1002/adma.200300381

Aizenberg, B. J., Lambert, G., Addadi, L., and Weiner, S. (1996). Stabilization of amorphous calcium carbonate. *Adv. Mater.* 8, 222–226. doi: 10.1002/adma.19960080307

Akiva-Tal, A., Kababya, S., Balazs, Y. S., Glazer, L., Berman, A., Sagi, A., et al. (2011). In situ molecular NMR picture of bioavailable calcium stabilized as amorphous CaCO3 biomineral in crayfish gastroliths. *Proc. Natl. Acad. Sci. U.S.A.* 108, 14763–14768. doi: 10.1073/pnas.1102608108

Allison, P. A. (1986). Soft-bodied animals in the fossil record: the role of decay in fragmentation during transport. *Geology* 14, 979–981. doi: 10.1130/0091-7613(1986)14<979:SAITFR>2.0.CO;2

Al-Sawalmih, A., Li, C., Siegel, S., Fratzl, P., and Paris, O. (2009). On the stability of amorphous minerals in lobster cuticle. *Adv. Mater.* 21, 4011–4015. doi: 10.1002/adma.200900295

Arias, J. L., and Fernandez, M. S. (2008). Polysaccharides and proteoglycans in calcium carbonate-based biomineralization. *Chem. Rev.* 108, 4475–4482. doi: 10.1021/cr078269p

Avnimelech, Y. (1983). Phosphorus and calcium carbonate solubilities in lake kinneret. *Limnology* 28, 640–645. doi: 10.4319/lo.1983.28.4.0640

Becker, A., Ziegler, A., and Epple, M. (2005). The mineral phase in the cuticles of two species of *Crustacea* consists of magnesium calcite, amorphous calcium carbonate, and amorphous calcium phosphate. *Dalt. Trans.* 2005, 1814–1820. doi: 10.1039/b412062k

Bentov, S., Aflalo, E. D., Tynyakov, J., Glazer, L., and Sagi, A. (2016). Calcium phosphate mineralization is widely applied in crustacean mandibles. *Sci. Rep.* 6:22118. doi: 10.1038/srep22118

Bentov, S., Weil, S., Glazer, L., Sagi, A., and Berman, A. (2010). Stabilization of amorphous calcium carbonate by phosphate rich organic matrix proteins and by single phosphoamino acids. *J. Struct. Biol.* 171, 207–215. doi: 10.1016/j.jsb.2010.04.007

Bentov, S., Zaslansky, P., Al-Sawalmih, A., Masic, A., Fratzl, P., Sagi, A., et al. (2012). Enamel-like apatite crown covering amorphous mineral in a crayfish mandible. *Nat. Commun.* 3:839. doi: 10.1038/ncomms1839

Blue, C. R., and Dove, P. M. (2015). Chemical controls on the magnesium content of amorphous calcium carbonate. *Geochim. Cosmochim. Acta* 148, 23–33. doi: 10.1016/j.gca.2014.08.003

Blue, C. R., Giuffre, A., Mergelsberg, S., Han, N., De Yoreo, J. J., and Dove, P. M. (2017). Chemical and physical controls on the transformation of amorphous calcium carbonate into crystalline CaCO3 polymorphs. *Geochim. Cosmochim. Acta* 196, 179–196. doi: 10.1016/j.gca.2016.09.004

Boßelmann, F., Romano, P., Fabritius, H., Raabe, D., and Epple, M. (2007). The composition of the exoskeleton of two crustacea: the american lobster *Homarus americanus* and the edible crab *Cancer pagurus*. *Thermochim. Acta* 463, 65–68. doi: 10.1016/j.tca.2007.07.018

Briggs, D. E. G., and Kear, A. J. (1994). Decay and mineralization of shrimps. *Palaios* 9, 431–456. doi: 10.2307/3515135

Briggs, D. E. G., and Wilby, P. R. (1996). The role of the calcium carbonate-calcium phosphate switch in the mineralization of soft-bodied fossils. *J. Geol. Soc. London* 153, 665–668. doi: 10.1144/gsjgs.153.5.0665

Busenberg, E., and Plummer, N. L. (1985). Kinetic and thermodynamic factors controlling the distribution of SO32- and Na+ in calcites and selected aragonites. *Geochim. Cosmochim. Acta* 49, 713–725. doi: 10.1016/0016-7037(85)90166-90168

Clarke, F. W., and Wheeler, W. C. (1922). *The Inorganic Constituents of Marine Invertebrates*. Washington D.C: U. S Gov't. Print. Off, doi: 10.5962/bhl.title.11289

Clarkson, J. R., Price, T. J., and Adams, C. J. (1992). Role of metastable phases in the spontaneous precipitation of calcium carbonate. *J. Chem. Soc. Faraday Trans.* 88, 243–249. doi: 10.1039/ft9928800243

Coblentz, F. E., Shafer, T. H., and Roer, R. D. (1998). Cuticular proteins from the blue crab alter in vitro calcium carbonate mineralization. *Comp. Biochem. Physiol. B* 121, 349–360. doi: 10.1016/S0305-0491(98)10117-10117

Cribb, B. W., Rathmell, A., Charters, R., Rasch, R., Huang, H., and Tibbetts, I. R. (2009). Structure, composition and properties of naturally occurring non-calcified crustacean cuticle. *Arthropod Struct. Dev.* 38, 173–178. doi: 10.1016/j.asd.2008.11.002

Dai, L., Cheng, X., and Gower, L. B. (2008). Transition bars during transformation of an amorphous calcium carbonate precursor. *Chem. Mater.* 20, 6917–6928. doi: 10.1021/cm800760p

Freitas, P. S., Clarke, L. J., Kennedy, H., Richardson, C. A., and Abrantes, F. (2006). Environmental and biological controls on elemental (Mg/Ca, Sr/Ca and Mn/Ca) ratios in shells of the king scallop *Pecten maximus*. *Geochim. Cosmochim. Acta* 70, 5119–5133. doi: 10.1016/j.gca.2006.07.029

Glusker, J. P. (1991). Structural aspects of metal liganding to functional groups in proteins. *Adv. Protein Chem.* 42, 1–76. doi: 10.1016/S0065-3233(08)60534-3

Glynn, J. P. (1968). Studies on the ionic, protein and phosphate changes associated with the moult cycle of *Homarus vulgaris*. *Comp. Biochem. Physiol.* 26, 937–946. doi: 10.1016/0010-406X(68)90013-3

Greenaway, P. (1985). Calcium balance and moulting in the *Crustacea*. *Biol. Rev.* 60, 425–454. doi: 10.1111/j.1469-185X.1985.tb00424.x

Grodowitz, M. J., Roseland, C. R., Hu, K. K., Broce, A. B., and Kramer, K. J. (1987). Mechanical properties of mineralized and sclerotized puparial cuticles of the flies *Musca autumnalis* and *M. domestica*. *J. Exp. Zool.* 243, 201–210. doi: 10.1002/jez.1402430205

Hammersley, A. P., Svensson, S. O., Thompson, A., Graafsma, H., Kvick, Å., and Moy, J. P. (1995). Calibration and correction of distortions in two-dimensional detector systems. *Rev. Sci. Instrum.* 66, 2729–2733. doi: 10.1063/1.1145618

Hayes, D. K., and Armstrong, W. D. (1961). The distribution of mineral material in the calcified carapace and claw shell of the american lobster, homarus americanus, evaluated by means of microroentgenograms. *Biol. Bull.* 121, 307–315. doi: 10.2307/1539435

Huner, J. V., Colvin, L. B., and Reid, B. L. (1979). Postmolt mineralization of the of juvenile california brown shrimp, *Penaeus Californiensis* (*Decapoda: Penaeidae*). *Comp. Biochem. Physiol.* 62A, 889–893. doi: 10.1016/0300-9629(79)90023-9

Hyžný, M., Schlögl, J., Charbonnier, S., Schweigert, G., Rulleau, L., and Gouttenoire, M. (2015). Intraspecific variation and taphonomy of a new erymid lobster (*Crustacea: Decapoda*) from the middle jurassic of belmont (Beaujolais, France). *Geobios* 48, 371–384. doi: 10.1016/j.geobios.2015.07.006

Klein, R. T., Lohmann, K. C., and Thayer, C. W. (1996). Bivalve skeletons record sea-surface temperature and d18O via Mg/Ca and 18O/16O ratios. *Geology* 24, 415–418. doi: 10.1130/0091-7613(1996)024<0415:BSRSST>2.3.CO;2

Kunkel, J. G., Nagel, W., and Jercinovic, M. J. (2012). Mineral fine structure of the american lobster cuticle. *J. Shellfish Res.* 31, 515–526. doi: 10.2983/035.031.0211

Levi-Kalisman, B. Y., Raz, S., Weiner, S., Addadi, L., and Sagi, I. (2002). Structural differences between biogenic amorphous calcium carbonate phases using X-ray absorption spectroscopy. *Adv. Funct. Mater.* 12, 43–48. doi: 10.1002/1616-3028(20020101)12

Loste, E., Wilson, R. M., Seshadri, R., and Meldrum, F. C. (2003). The role of magnesium in stabilising amorphous calcium carbonate and controlling calcite morphologies. *J. Cryst. Growth* 254, 206–218. doi: 10.1016/S0022-0248(03)01153-9

Marlowe, R. L., Dillaman, R. M., and Roer, R. D. (1994). Lectin binding by crustacean cuticle: the cuticle of *Callinectes sapidus* throughout the molt cycle, and the intermolt cuticle of *Procambarus clarkii* and *Ocypode quadrata*. *J. Crustac. Biol.* 14, 231–246. doi: 10.2307/1548904

Martill, D. M. (1990). Macromolecular resolution of fossilized muscle tissue from an elopomorph fish. *Nature* 346, 171–172. doi: 10.1038/346171a0

Michel, F. M., MacDonald, J., Feng, J., Phillips, B. L., Ehm, L., Tarabrella, C., et al. (2008). Structural characteristics of synthetic amorphous calcium carbonate. *Chem. Mater.* 20, 4720–4728. doi: 10.1021/cm800324v

Mutel, M. H. E., Waugh, D. A., Feldmann, R. M., and Parsons-Hubbard, K. M. (2008). Experimental taphonomy of *Callinectes sapidus* and cuticular controls on preservation. *Palaios* 23, 615–623. doi: 10.2110/palo.2008.p08-024r

Neues, F., Ziegler, A., and Epple, M. (2007). The composition of the mineralized cuticle in marine and terrestrial isopods: a comparative study. *CrystEngComm* 9, 1245–1251.

Qi, C., Zhu, Y., and Chen, F. (2014). Microwave hydrothermal transformation of amorphous calcium carbonate nanospheres and application in protein adsorption. *ACS Appl. Mater. Interfaces* 6, 4310–4320. doi: 10.1021/am4060645

Qiu, X., Thompson, J. W., and Billinge, S. J. L. (2004). PDFgetX2: a GUI-driven program to obtain the pair distribution function from X-ray powder diffraction data. *J. Appl. Crystallogr.* 37:678. doi: 10.1107/S0021889804011744

Reddy, M. M. (1977). Crystallization of calcium carbonate in the presence of trace concentrations of phosphorus-containing anions. I. Inhibition by phosphate and glycerophosphate ions at pH 8.8 and 25°C. *J. Cryst. Growth* 41, 287–295. doi: 10.1016/0022-0248(77)90057-4

Richards, A. G. (1951). *The Integument of Arthropods: the Chemical Components and their Properties, the Anatomy and Development, and the Permeability*. Minneapolis, MN: University of Minnesota Press.

Roer, R., and Dillaman, R. (1984). The structure and calcification of the crustacean cuticle. *Am. Zool.* 24, 893–909. doi: 10.1093/icb/24.4.893

Roseland, C. R., Grodowitz, M. J., Kramer, K. J., Hopkins, T. L., and Broce, A. B. (1985). Stabilization of mineralized and sclerotized puparial cuticle of *muscid* flies. *Insect Biochem.* 15, 521–528. doi: 10.1016/0020-1790(85)90065-4

Rütt, U., Beno, M. A., Strempfer, J., Jennings, G., Kurtz, C., and Montano, P. A. (2001). Diffractometer for high energy X-rays at the APS. *Nucl. Instrum. Methods Phys. Res. A* 46, 1026–1029. doi: 10.1016/S0168-9002(01)00580-0

Sato, A., Nagasaka, S., Furihata, K., Nagata, S., Arai, I., Saruwatari, K., et al. (2011). Glycolytic intermediates induce amorphous calcium carbonate formation in crustaceans. *Nat. Chem. Biol.* 7, 197–199. doi: 10.1038/nchembio.532

Sawada, K. (1997). The mechanisms of crystallization and transformation of calcium carbonates. *Pure Appl. Chem.* 69, 921–928. doi: 10.1351/pac199769050921

Soejoko, D. S., and Tjia, M. O. (2003). Infrared spectroscopy and X ray diffraction study on the morphological variations of carbonate and phosphate compounds in giant prawn (*Macrobrachium rosenbergii)* skeletons during its moulting period. *J. Mater. Sci.* 38, 2087–2093. doi: 10.1023/A:1023566227836

Travis, D. F. (1963). Structural features of mineralization from tissue to macromolecular levels of organization in the decapod *Crustacea. Ann. N. Y. Acad. Sci.* 109, 177–245. doi: 10.1111/j.1749-6632.1963.tb13467.x

Tsujita, C. J. (2003). Smothered scampi: taphonomy of lobsters in the upper cretaceous bearpaw formation, southern alberta. *J. Taphon.* 1, 187–206.

Vigh, D. A., and Dendinger, J. E. (1982). Temporal relationships of postmolt deposition of calcium, magnesium, chitin and protein in the cuticle of the atlantic blue crab, *Callinectes sapidus* rathbun. *Comp. Biochem. Physiol.* 72, 365–369. doi: 10.1016/0300-9629(82)90232-8

Vijayan, K. K., and Diwan, A. D. (1996). Fluctuations in Ca, Mg and P levels in the hemolymph, muscle, midgut gland and exoskeleton during the moult cycle of the Indian white prawn, *Penaeus indicus* (*Decapoda: Penaeidae*). *Comp. Biochem. Physiol. A Physiol.* 114, 91–97. doi: 10.1016/0300-9629(95)02096-9

Wood, S., and Russell, J. D. (1987). On the nature of the calcium carbonate in the exoskeleton of the woodlouse *Oniscus asellus* L. *(Isopoda, Oniscoidea). Crustaceana* 53, 49–53. doi: 10.1163/156854087X00619

Xu, A. W., Yu, Q., Dong, W. F., Antonietti, M., and Cölfen, H. (2005). Stable amorphous CaCO3 microparticles with hollow spherical superstructures stabilized by phytic acid. *Adv. Mater.* 17, 2217–2221. doi: 10.1002/adma.200500747

Ziegler, A. (2008). The cationic composition and pH in the moulting fluid of *Porcellio scaber* (*Crustacea, Isopoda*) during calcium carbonate deposit formation and resorption. *J. Comp. Physiol. B* 178, 67–76.

Conflict of Interest Statement: The authors declare that the research was conducted in the absence of any commercial or financial relationships that could be construed as a potential conflict of interest.